NUMERICAL PREDICTION OF FORCED-IGNITION LIMIT IN HIGH-PRESSURIZED HYDROGEN JET FLOW THROUGH A PINHOLE

Asahara, M.[1], Tsuboi, N.[2], Fujimoto, K. [3], Muto, D.[4] and Hayashi, A.K. [5]

[1] Mechanical Engineering, Gifu University, 1-1 Yanagido, Gifu, Gifu, 501-1193, Japan, asahara@gifu-u.ac.jp

[2] Mechanical Engineering, Kyushu Institute of Technology, 1-1 Sensui-cho, Tobata, Kitakyushu, Fukuoka, 804-8550, Japan, tsuboi@mech.kyutech.ac.jp

[3] Mechanical Engineering, Kyushu Institute of Technology, 1-1 Sensui-cho, Tobata, Kitakyushu, Fukuoka, 804-8550, Japan, meteor9150@gmail.com

[4] Japan Aerospace Exploration Agency, Tsukuba, Ibaraki, 305-8505, Japan, muto.daiki@jaxa.jp

[5] Mechanical Engineering, Aoyama Gakuin University, 5-10-1 Fuchinobe, Chuo, Kanagawa, 252-5258, Japan, hayashi@aoyama.me.jp

ABSTRACT

The numerical simulations on the high-pressure hydrogen jet are performed by using the unsteady three-dimensional compressible Navier-Stokes equations with multi-species conservation equations. The present numerical results show that the highly expanded hydrogen free jet observes and the distance between the Mach disc and the nozzle exit agrees well with the empirical equation. The time-averaged H_2 concentration of the numerical simulations agrees well with the experimental data and the empirical equation. The numerical simulation of ignition in a hydrogen jet is performed to show the flame behaviour from the calculated OH isosurface. We predicted the ignition and no-ignition region from the present numerical results about the forced ignition in the high-pressurized hydrogen jet.

1 INTRODUCTION

Hydrogen is attracting interest as an alternate fuel to fossil fuels. The Government of Japan in particular is aiming to create a hydrogen energy society as part of its national growth strategy, and its Basic Act on Energy Policy specifies concrete goals to realize a hydrogen energy society. As part of this movement, in 2014, Toyota Motor Corporation led the world by starting general sales of a fuel cell vehicle (FCV) powered by hydrogen, and Honda Motor Company started to lease FCVs in 2016. In this way, Japan is leading the world in the sale of FVC, but is behind Europe and North America in the establishment of a hydrogen supply infrastructure, resulting in a bottleneck delaying the establishment of the hydrogen energy society. It is suggested that the reason for this delay is anxiety about hydrogen resulting from inadequate evaluation of its risks. In order to overcome this problem to realize the creation of a hydrogen energy society, it is necessary to accurately assess the risks of hydrogen and take measures to prevent explosions and to mitigate the damage they would cause.

As FCVs have become commercially available, the demand for hydrogen fuel and its installation are expected to expand, in future. As a hydrogen energy society is probable in future, it is necessary to investigate the fundamental properties of hydrogen. Hydrogen is a light gas and is the most diffusive among all the gases; it is flammable and its ignition energy of 0.02 mJ is considerably low. The lower and higher flammable limits of hydrogen in air are 4% and 75% in mole fraction, respectively. When the stored hydrogen leaks due to breaks in the pipes or tanks, it disperses unsteadily within a short time. Then, the flammable region of the hydrogen/air mixture expands over a wide range. If an ignition source exists in the region of the leaked hydrogen, an explosion can occur. Hence, in order to prevent an accident owing to hydrogen leakage from a stored tank, it is necessary to understand the flow dynamics of the hydrogen dispersion and to set up an appropriate standard and control for the hydrogen properties.

Ignition in a jet flow, investigated in 1981 by Birch et al. [1], has shown that the calculated mole concentration at the lower flammability limit in a natural gas jet does not agree with that at the lower flammability limit in a static condition. They also reported that it was possible to predict the ignition condition from the average concentration data, although the average concentration could not be related to the ignition limit, in the case of combustion. Swain et al. [2,3] experimentally demonstrated that the hydrogen gas concentration near the ignition boundary does not agree with the combustible limit of 4 %, under a static condition. They also showed that the ignition condition in the jet depended upon the ignition energy of the spark plug and the spark plug gap; it was difficult to measure the mole concentration accurately at the ignition location and the minimum mole concentration at ignition was approximately 5–10 %. Hydrogen jet and combustion studies are mostly performed experimentally [4,

5, 6, 7] with few numerical simulations.

This study simulates the injection of a high-pressure hydrogen supersonic free jet into the atmosphere to understand the unsteady dispersion process.

2 NUMERICAL METHOD

The governing equations are the unsteady three-dimensional compressible Navier-Stokes equations, which include the conservation laws of mass, momentum, and energy, and the species conservation of nine chemical species, (H_2, O_2, H, O, OH, HO_2, H_2O_2, H_2O, N_2). The AUSMDV [8] is adopted for the inviscid flux. A second-order MUSCL with a minmod limiter is used. The viscous term is the second-order central difference. The LU-SGS implicit method [9] is used for time integration and the number of inner iterations is set to three for preserving the time accuracy. The SA model is adopted as the turbulent model [10]. The UT-JAXA model [11] is used for chemical kinetics to solve the ignition problem.

The numerical grid systems used are shown in Figs. 1–3. The nozzle exit diameter, d_e, is 0.2 mm. The details of these grids are summarized in Table 1. In Grid 1, the grid width in the stream-wise direction, Δx, gradually increases from the nozzle exit to the location of the Mach disc. Δx behind the Mach disc is set to 0.5 mm. Δx for Grid 2 is changed from 0.06 mm to 3.5 mm in order to calculate the hydrogen concentration at a distance from the nozzle exit. Grid 3 is used to calculate the ignition and combustions with Grid 2. The centre-line of grid 3 locates at x = 212 mm on the symmetry axis.

Table 1. Summary of computational grid systems.

	Grid 1	Grid 2	Grid 3(ignition region)
Number of grid points	497(axial) ×65(circumferential) ×361(radial)	873(axial) ×35(circumferential) ×361(radial)	161 × 65 ×161
x/d_e	300	2600	See Fig. 3
r/d_e	170	1060	
Δx_{min} [mm]	0.05	0.06	
Δx_{max} [mm]	0.5	3.5	
Δr_{min} [mm]	0.02	0.04	

Table 2. Summary of simulation conditions.

	Injection	Ambient
Mixture Gas	H_2	Air (O_2:N_2 = 0.244:0.756)
Density [kg/m^3]	ρ_j = 42.1	ρ_0 = 1.177
Temperature [K]	T_j = 249	T_0 = 300
Pressure [MPa]	P_j = 43.2	P_0 = 0.1
Velocity [m/s]	u_j = 1203	u_0 = 0
Mach number	1.0	0
Reynolds number based on d_e	1.3 x 10^6	

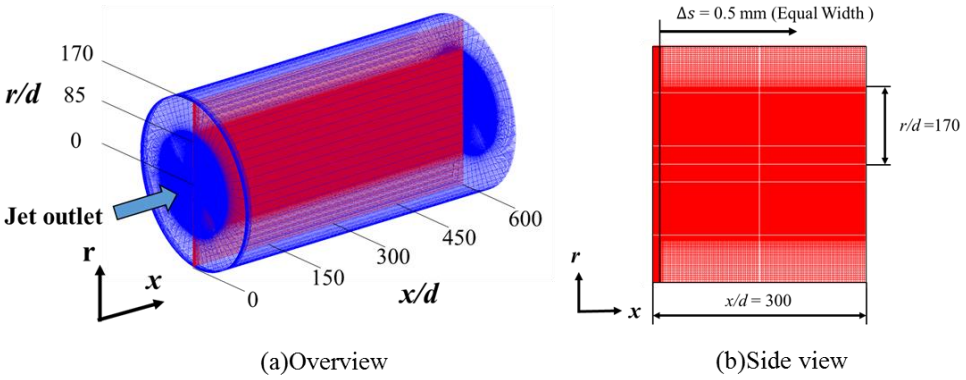

Figure 1. Computational grid system (Grid 1).

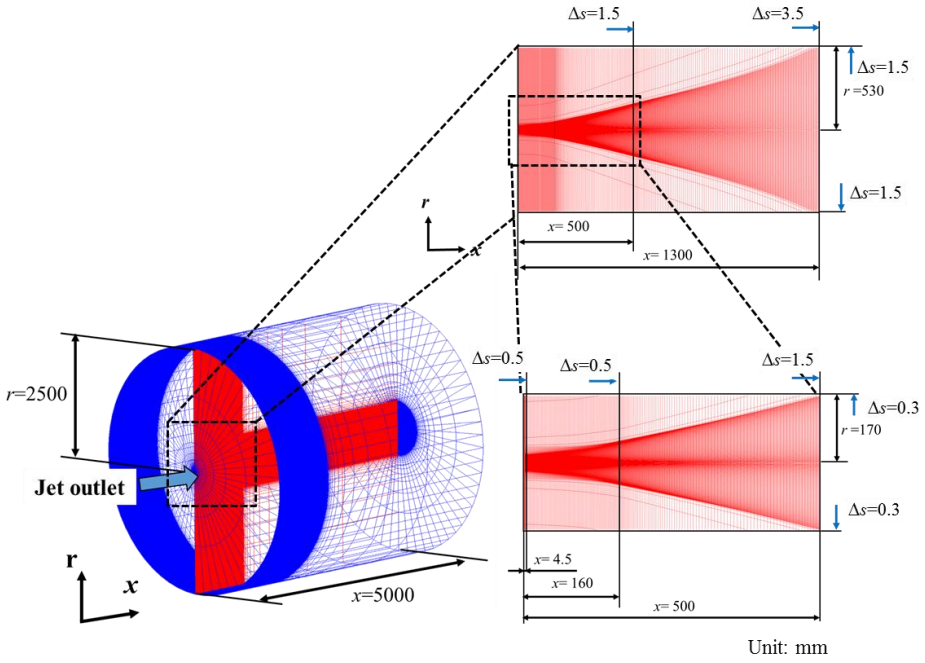

Figure 2. Computational grid system (Grid 2). d_e=0.4 mm.

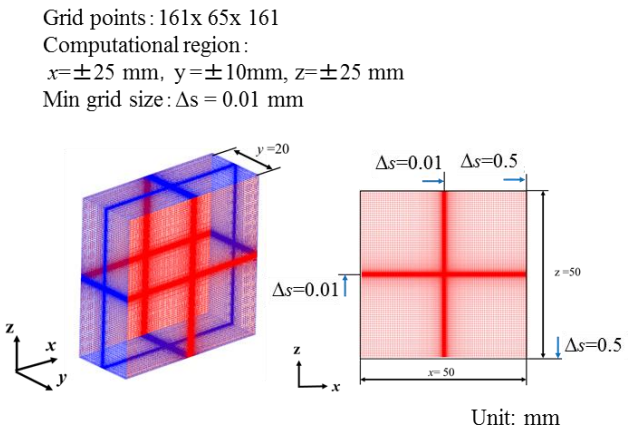

Figure 3. Computational grid system (Grid 3).

3.0 RESULTS AND DISCUSSION

3.1 Hydrogen dispersion behavior

Figure 4 shows the snapshot of H_2 flow for Grid 1. Unsteady flow and Mach disc are observed by Fig. 4 (a) and (b), respectively. The numerical Mach disc height, $X_{m,num}$, is 3.5 mm and it agrees well with the semi-experimental Mach disc height, $X_{m,exp.}$=3.83, predicted by an empirical equation [12],

$$X_{m,exp.}/D_e=0.67(p_0/p_b)^{0.5},$$

where D_e is the nozzle exit diameter, p_0 is the stagnation pressure, and p_b is the background pressure, respectively. The supersonic flow behind the Mach disc is disturbed into the atmospheric pressure. The barrel shock, Mach disc, and shear layer are formed behind the nozzle exit as shown in Fig. 4(b). The H_2 concentration is 100% in the barrel shock and shear layer from nozzle to the location of x/d=300 (x=60mm). The hydrogen concentration decrease behind the location of x/d=300 (x=60mm). It indicates that hydrogen mixes with the air by momentum diffusion effect at the region away from x/d=300 (x=60mm).

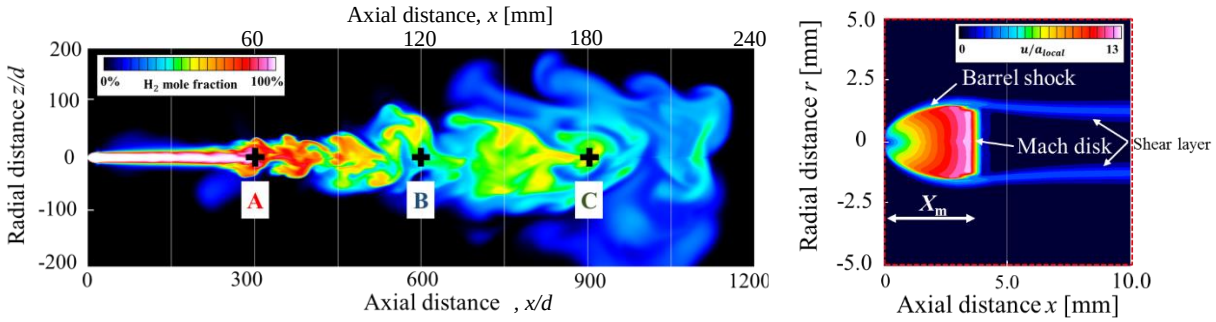

(a) Overview (b) Enlargement view near nozzle

Figure 4. Snapshot of H_2 flow for Grid 1. (a) Distribution of H_2 concentration, and (b) distribution of local Mach number near nozzle.

Figure 5 shows the distribution of the present numerical time-averaged hydrogen concentration along the symmetric axis compeered with experimental one [4,12]. The distance from nozzle is normalized by the effective diameter which is defined by the following equation:

$$\theta = d_e\left(\frac{\rho_*}{\rho_b}\right)^{0.5} = \sqrt{\left(\frac{2}{\gamma+1}\right)^{\frac{1}{\gamma-1}}\frac{p_0}{R_{H_2}T_0}\frac{R_{air}T_b}{p_b}}$$

Where ρ_* is density at nozzle exit, subscripts b and 0 are background state and stagnation state, respectively. This figure indicates that the present numerical results agree well with the empirical equation ($4800/x(x/\theta)$) and experimental data [4,13]. The experimental hydrogen concentration for x/θ >2000 is larger than the empirical equation because the hydrogen jet flow is affected by the buoyancy.

Figure 6 shows instantaneous hydrogen concentration at (x/d, r/d) = (300, 0), (600, 0), and (900, 0). The hydrogen concentrations at these points fluctuate and it has lower frequency with distance from nozzle, because the hydrogen jet has unsteady complex vortices.

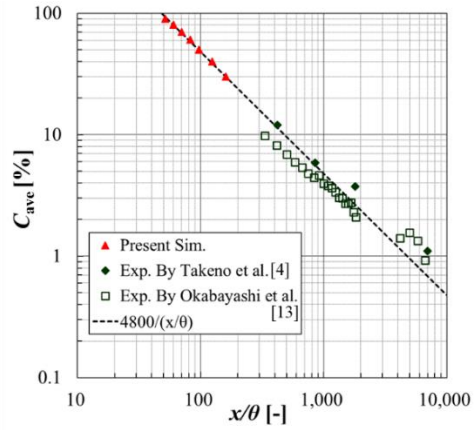

Figure 5. Time-averaged H_2 mole fraction along axis.

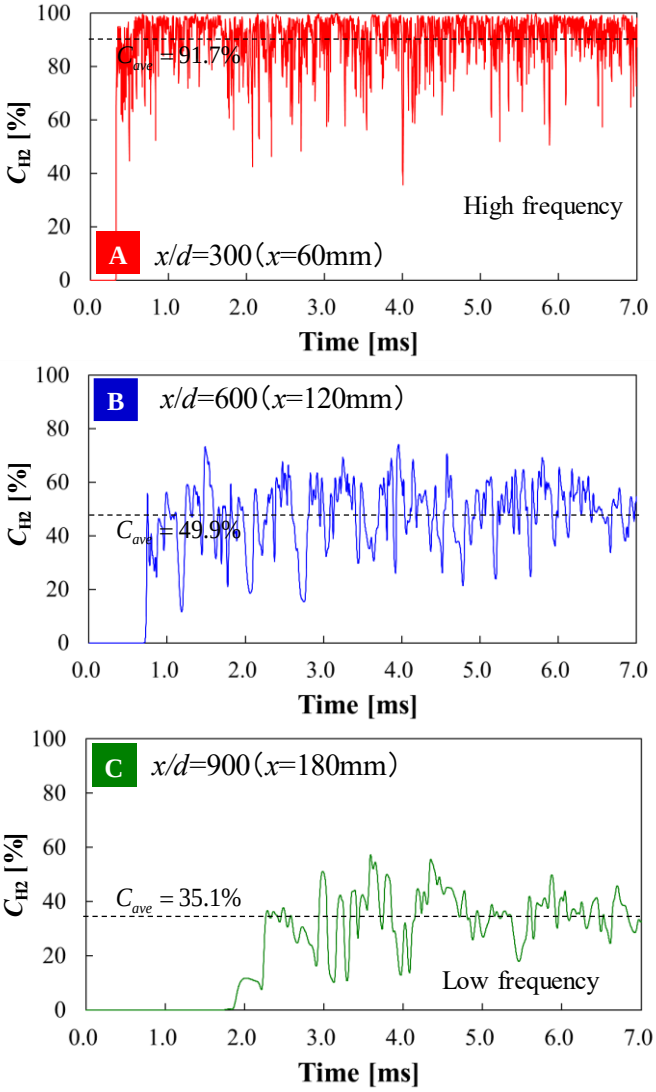

Figure 6. Time histories of H_2 concentration at x/d =300 (x=60mm), x/d =600 (x=120mm), and x/d =900 (x=180mm).

3.2 Flame behavior

The numerical simulation of ignition in the hydrogen jet is performed in the next step. The computational grids are shown in Figs. 2 and 3. The ignition size, pressure, and temperature are 0.2 mm, 2 MPa, and 3078 K (adiabatic flame temperature), respectively. The mass fractions of the chemical species are calculated under an equilibrium state for 2 MPa and 3078 K. In the present study, the forced ignition point at (x/d, r/d) = (1000, 0), (4450, 0), and (6250, 0).

Figure 7 shows the time series of instantaneous OH isosurface on the hydrogen concentration distribution after forced ignition at x/d =1000 (x=200mm). The OH isosurface indicates flame front. The flame under this condition develops to downstream and upstream along high hydrogen concentration region, and after that flame stays around near nozzle (jet flame). Figure 8 shows time history of flame tip location and flame length at x/d =1000 (x=200mm). The flame spreads rapidly to upstream and downstream until 3msec after ignition, and it has slow growth rate after 3msec.

Figure 9 shows the time series of instantaneous OH isosurface on the hydrogen concentration distribution after forced ignition at x/d =4450 (x=890mm). The flame under this condition develops to downstream and it goes into a gradual decline from breakup at upstream part. Figure 10 shows time history of flame tip location and flame length at x/d =4450 (x=890mm). The flame spreads until 3msec after ignition as well as the case of forced ignition at x/d =1000 (x=200mm) (as shown in Fig. 8). However, the flame tip of upstream does not ran back to nozzle after 3msec, and it might go to extinction after breakup. The maximum flame length in this case is about 300mm at 10msec after ignition.

Figure 11 shows the time series of instantaneous OH isosurface on the hydrogen concentration distribution after forced ignition at x/d =6250 (x=1250mm). The flame core does not germinate Figure 12 shows time history of flame length at x/d =6250 (x=1250mm). The maximum flame length in this case is about 32mm at 2msec after ignition.

3.3 Ignition limit

Lower flammable concentration of hydrogen (=4%) is defined by the experiment that the forced ignition test sparked under the static premixed condition at the 2/3 times length of the diameter from bottom in the 5L spherical vessel (about 150mm). If the flame touches to the upper or side wall of spherical vessel, ignition under that concentration is regarded as success [14]. It indicates that “the ignition” is equal to the self-sustained reaction without influence of forced ignition energy. Therefore, the ignition under dynamic diffusion mixed condition is defined by the flame length for the self-sustained reaction. If the flame length is over than 150mm (which is referred by the paper [14]), the ignition under dynamic diffusion mixed condition success.

Figure 13 shows the flame length and the time averaged hydrogen concentration along the symmetric axis. The flame length is short with the distance from the nozzle to the igniter. In this figure, we get the forced ignition limit in 82MPa hydrogen jet = 1100mm.

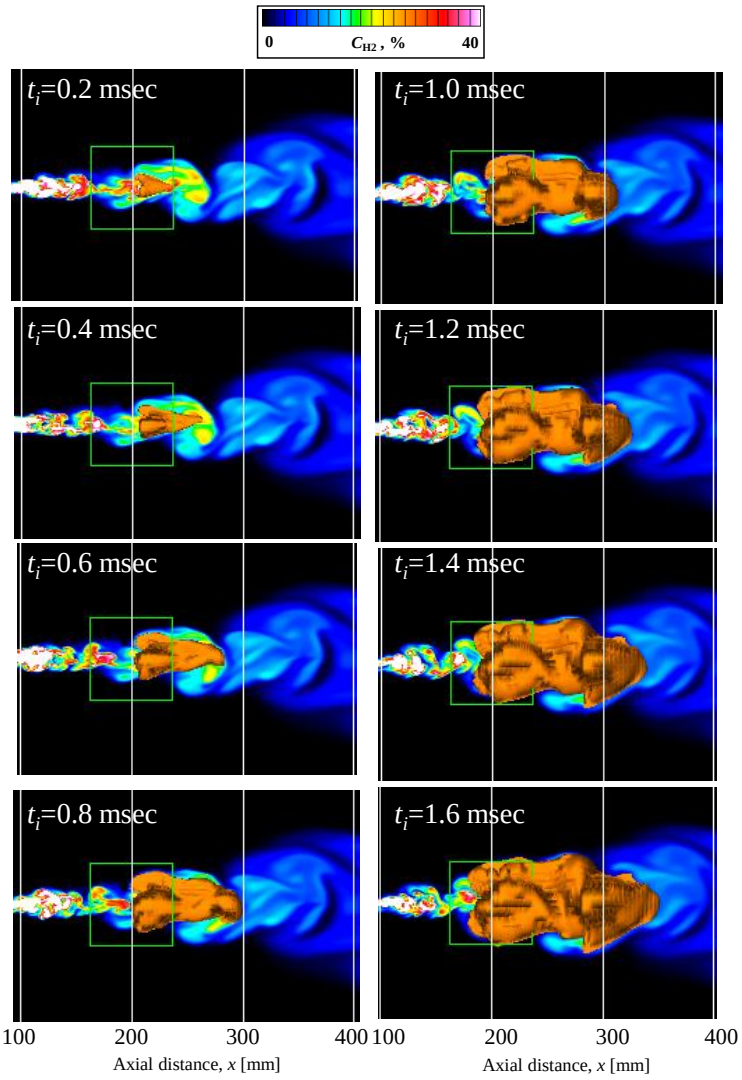

Figure 7. Time series of instantaneous H_2 concentration distribution and OH isosurface (orange surface) after forced ignition at x/d =1000 (x=200mm).

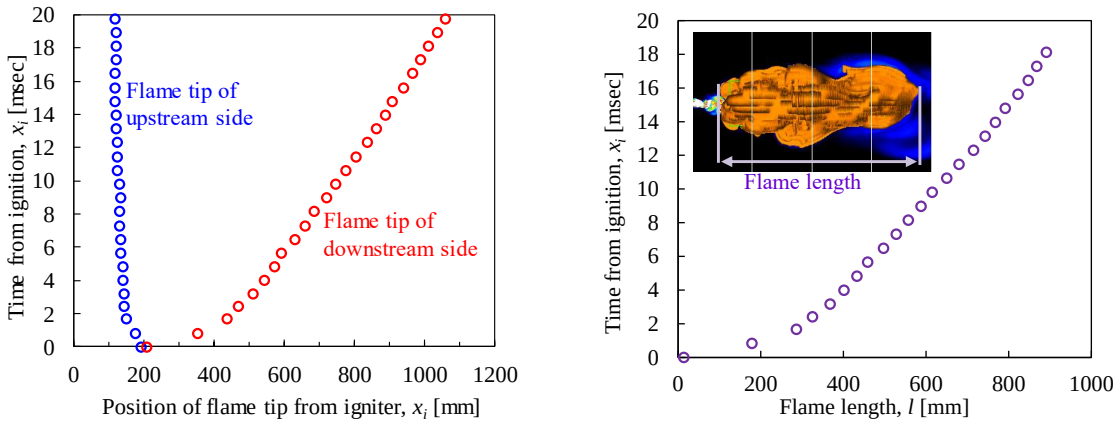

(a) position of flame tip (b) Flame length

Figure 8. Flame behavior after forced ignition at x/d =1000 (x=200mm). Time history of (a) the position of flame tip and (b) the flame length.

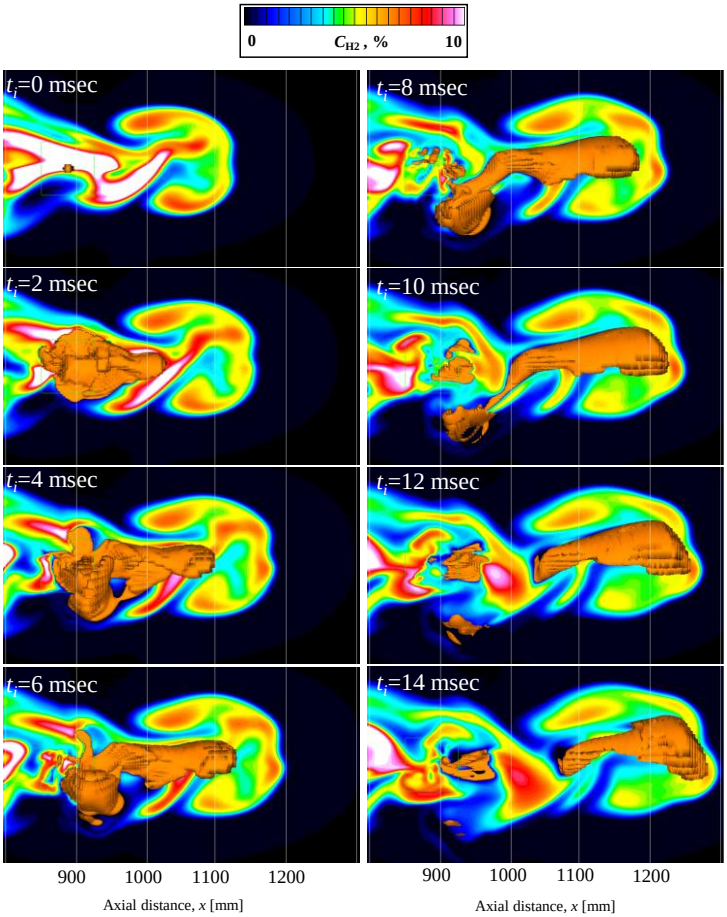

Figure 9. Time series of instantaneous H_2 concentration distribution and OH isosurface (orange surface) after forced ignition at x/d =4450 (x=890mm).

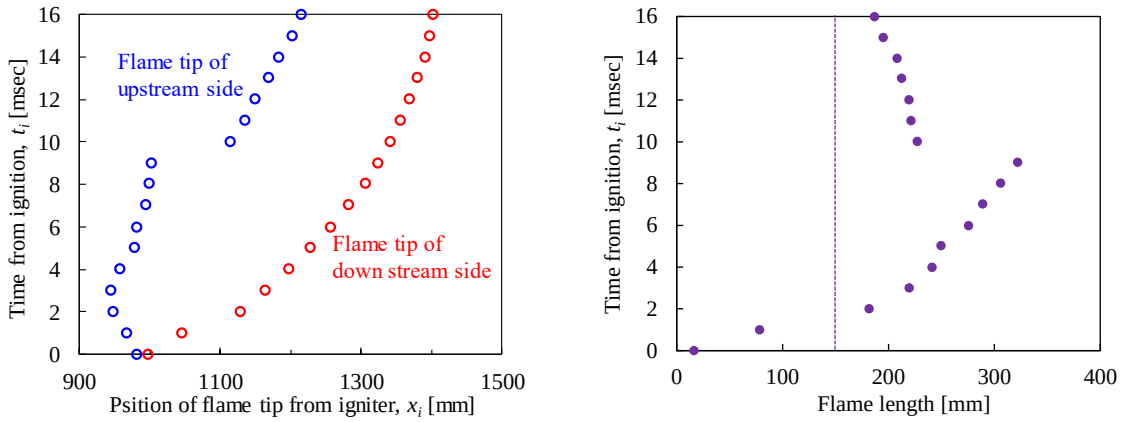

(a) position of flame tip (b) Flame length

Figure 10. Flame behavior after forced ignition at x/d =4450 (x=890mm). Time history of (a) the position of flame tip and (b) the flame length.

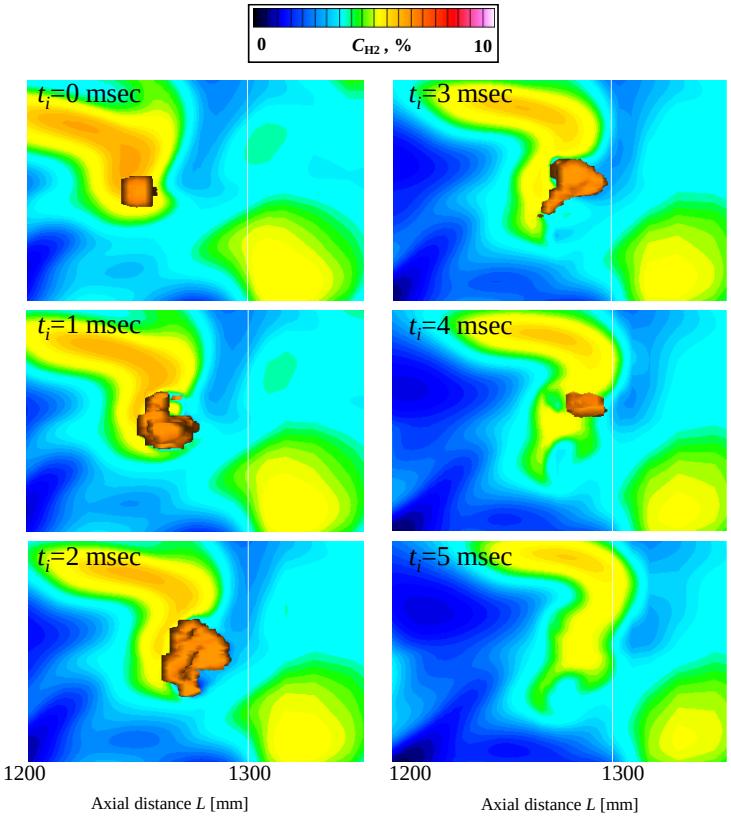

Figure 11. Time series of instantaneous H_2 concentration distribution and OH isosurface (orange surface) after forced ignition at x/d =6250 (x=1250mm).

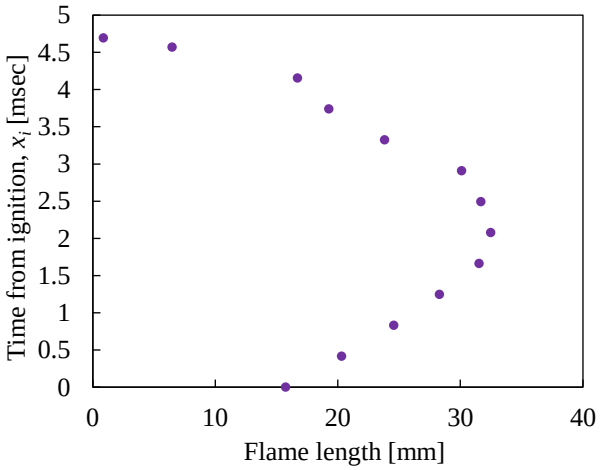

Figure 12. Time history of the flame length after forced ignition at x/d =6250 (x=1250mm).

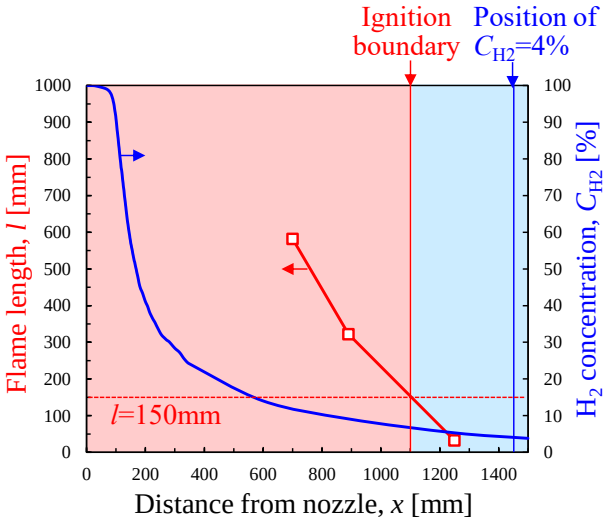

Figure 13. The flame length and the time averaged H_2 concentration along the symmetric axis.

4 CONCLUDIONS

The numerical simulation of a high-pressurized hydrogen jet using the unsteady three-dimensional compressible Navier-Stokes equations along with the multi-species conservation equations was conducted in this study. The numerical results demonstrate that the highly expanded hydrogen free jet observes and that the distance between the Mach disc and nozzle exit agrees well with the empirical equation. The time-averaged hydrogen concentration of the numerical simulation agrees well with the experimental data and the empirical equation. The numerical simulation of ignition in a hydrogen jet is performed to show the flame behaviour from the calculated OH isosurface. We predict the ignition and no-ignition region from the present numerical results about the forced ignition in the high-pressurized hydrogen jet.

5 ACKNOWLEDGEMENTS

This research was done in collaboration with Cybermedia Center using the Osaka University supercomputer system. This study is supported by the New Energy and Industrial Technology Development Organization of Japan (NEDO) under the project “Research and Development of Technology for Hydrogen Utilization”.

REFERENCES

1. Birch, A.D., Brown, D.R. and Dodson, M.G., “Ignition Probabilities in Turbulent Mixing Flows,” 18th International Symposium on Combustion, pp. 1775-1780, (1981).
2. Swain, M.R., Filoso, P.A. and Swain, M.N., “Ignition of lean hydrogen-air mixtures,” International Journal of Hydrogen Energy, 30, pp. 1447-1455, (2005).
3. Swain, M.R., Filoso, P.A. and Swain, M.N., “An experimental investigation into the ignition of leaking hydrogen,” International Journal of Hydrogen Energy, 32, pp. 287-295, (2007).
4. Takeno, K., Okabayashi, K., Kouchi, A., Nonaka, T., Hashiguchi, K. and Chitose, K., “Dispersion and explosion field tests for 40 MPa pressurized hydrogen,” International Journal of Hydrogen Energy, 32, pp. 2144-2153, (2007).
5. Houf, W.G., Evans, G.H. and Schefer, R.W., “Analysis of jet flames and unignited jets from unintended releases of hydrogen,” International Journal of Hydrogen Energy, 34, pp. 5961-5969, (2009).

6. Khaksarfard, R. and Paraschivoiu, M., “Numerical simulation of high pressure hydrogen release through an expanding opening,” International Journal of Hydrogen Energy, 37, pp. 8734-8743, (2012).
7. Wang, C.J., Wen, J.X., Chen, Z.B. and Dembele, S., “Predicting radiative characteristics of hydrogen and hydrogen/methane jet fires using FireFORM,” International Journal of Hydrogen Energy, 39, pp. 20560-20569, (2014).
8. Wada, Y., and Liou, M., “A Flux Splitting Scheme with High Resolution and Robustness for Discontinuities,” AIAA Paper 94-0083, (1994).
9. Yoon, S., and Jameson, A., “Lower-Upper Symmetric-Gauss-Seidel Method for the Euler and Navier-Stokes Equations,” AIAA Journal, Vol. 26, No. 9, pp. 1025-1026, (1998).
10. Spalart, P., and Allmaras, S., “A One-Equation Turbulence Model for Aerodynamic Flows,” 30th Aerospace Sciences Meeting and Exhibit, AIAA 1992-0439, (1992).
11. K.Shimizu, H.Hibi, M.Koshi, M.Morii, N.Tsuboi, “An Updated Kinetic Mechanism for High-Pressure Hydrogen Combustion,” Journal of Propulsion and Power, Volume 27, Number 2, pp. 383-395, (2011).
12. Ashkenas, H., Sherman, F.S., “The Structure and Utilization of Supersonic Free Jets in Low Density Wind Tunnel,” Advances in Applied Mechanics-Rarefied Gas Dynamics. New York: Academic Press; 1965. pp. 84-105.Ashkenas, (1966).
13. Okabayashi, K., Tagashira, K., Takeno, K., Asahara, M., Hayashi, A.K., Komori, M., “Non-steady Characteristics of Dispersion and Ignitability for High-Pressureized Hydrogen Jet,” 54th Combustion Symposium(Japan), D231, (2016).
14. ASTM E681-09, “Standard test method for concentration limits of flammability of chemicals (vapors and gases),” (2009).